Communication

Spinel Ferrite/MnO Core/Shell Nanoparticles: Chemical Synthesis of All-Oxide Exchange Biased Architectures

Ombretta Masala, and Ram Seshadri

J. Am. Chem. Soc., **2005**, 127 (26), 9354-9355• DOI: 10.1021/ja051244s • Publication Date (Web): 09 June 2005

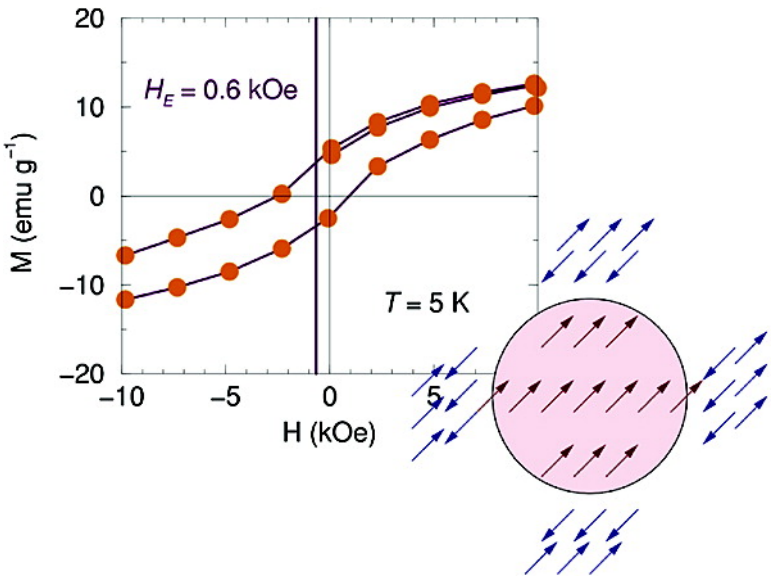

More About This Article

Additional resources and features associated with this article are available within the HTML version:

- Supporting Information
- Links to the 11 articles that cite this article, as of the time of this article download
- Access to high resolution figures
- Links to articles and content related to this article
- Copyright permission to reproduce figures and/or text from this article

View the Full Text HTML

J|A|C|S
COMMUNICATIONS

Published on Web 06/09/2005

Spinel Ferrite/MnO Core/Shell Nanoparticles: Chemical Synthesis of All-Oxide Exchange Biased Architectures

Ombretta Masala and Ram Seshadri*

Materials Department and Materials Research Laboratory, University of California, Santa Barbara, California 93106

Received February 27, 2005; E-mail: seshadri@mrl.ucsb.edu

Exchange coupling between ferromagnetic (FM) and antiferromagnetic (AFM) phases in composite materials is of great interest for technological applications. These materials find extensive use as read-heads in modern high-density magnetic storage disks.[1] FM−AFM exchange coupling was first observed in 1956 by Meiklejohn and Bean[2] in partially oxidized Co nanoparticles (10−100 nm). They observed that when the particles were field-cooled across the Néel temperature (T_N) of CoO an exchange bias occurred, which resulted in a shifted hysteresis loop and increased coercivity. Exchange bias has been since observed in other fine particle systems in which native particles have been partially oxidized, such as Ni−NiO, Fe−FeO, and Fe−Fe_3O_4.[3] Exchange bias has been studied more extensively in thin films because most of the technological applications which exploit this phenomenon make use of materials in the form of thin films. Examples include Fe_3O_4/CoO, Fe_3O_4/NiO, Fe/FeF_2, and FeNiB/CoO bilayers.[3−5] In recent years, many applications, such as high-density information storage, have required materials not only with tunable magnetic properties but also with reduced sizes, sparking a renewed interest in exchange-biased nanoparticles. Skumryev et al.[6] observed exchange bias in partially oxidized 4 nm Co nanoparticles embedded in an AFM CoO matrix. The FM−AFM magnetic coupling at the particle/matrix interface also led to an increase of the blocking temperature of the nanoparticles, resulting in an improved thermal stability. Large exchange bias was also observed in carbon-encapsulated and partially oxidized Co nanoparticles.[7] Interest in the Co/CoO system is due to high coercivity, large exchange bias, and magnetoresistance. The development of new routes for the synthesis of magnetic nanoparticles[8] has inspired complex composite FM−AFM nanostructures from alternative materials other than partially oxidized metal nanoparticles.

In this communication, we report the synthesis and characterization of high-quality core/shell nanoparticles where the ferrimagnetic core of a spinel ferrite $CoFe_2O_4$ is coated with a shell of the antiferromagnet MnO. The nanoparticles are obtained in the form of powders and are capped with organic surfactants which make them soluble in a range of organic solvents, opening a number of possibilities for further functionalization and processing.

$CoFe_2O_4$/MnO nanoparticles were synthesized by combining a high-temperature decomposition route with seed-mediated growth. Briefly, 5 nm $CoFe_2O_4$ nanoparticles were first synthesized by decomposing at high temperatures (∼300 °C) the acetylacetonate (acac) salts, $Co(acac)_2$ and $Fe(acac)_3$, in benzyl ether in the presence of 1,2-hexadecandiol and with oleic acid and oleylamine as capping agents.[9] Spinel ferrite nanoparticles prepared with this route are highly crystalline, monodispersed, and exhibit good magnetic properties.[10] The MnO shell was overgrown by mixing a hexane solution of the $CoFe_2O_4$ nanoparticles with dry $Mn(CH_3CO)_2$ and oleic acid in trioctylamine and heating the resulting mixture at 320 °C for 1 h, as described Yin and O'Brien.[11] Nanoparticles with nominal $CoFe_2O_4$:MnO molar ratios of 1:1, 3:1, and 6:1 were synthesized by varying accordingly the amounts of starting reagents. Similar reactions were also carried out to prepare $ZnFe_2O_4$/MnO nanostructures (see Supporting Information). The nanoparticles were characterized by X-ray powder diffraction (XRD) carried out on a Scintag PAD-X2 diffractometer with Cu Kα radiation (λ = 1.518 Å); transmission electron microscopy (TEM) was carried out at an accelerating voltage of 200 keV on a JEOL2010; magnetic measurements were carried out on a Quantum Design MPMS 5XL SQUID magnetometer.

Figure 1 shows a typical XRD pattern of $ZnFe_2O_4$/MnO nanoparticles with a nominal core/shell ratio of 6:1 exhibiting peaks that match with the reflections of cubic rock salt MnO and of the spinel ferrite $ZnFe_2O_4$. Corresponding XRD data on the $CoFe_2O_4$/MnO samples are very noisy due to fluorescence. TEM indicated that the nanoparticles are highly crystalline, monodisperse, with spherical shape and average total size of 8 nm. This is shown in Figure 2a for $CoFe_2O_4$/MnO nanoparticles. High-resolution TEM confirmed the core/shell structure of the nanoparticles (Figure 2b). The core appears with a darker contrast than the shell due to the difference in electron penetration efficiency arising from the distinct structure types. It should be noted that (a) the structures are not single nanocrystals, and (b) there is no evidence of epitaxy between core and shell. Also, such core/shell contrast differences are not noted in all particles. The $CoFe_2O_4$ core has a diameter of approximately 4−5 nm surrounded by the MnO shell with an average thickness of 2−3 nm for a total average particle size between 7 and 9 nm.

The magnetic properties of the nanoparticles were studied by measuring the magnetization as a function of temperature and field. Figure 3a−c shows the field-cooled (FC, solid) and zero-field-cooled (ZFC, dashed) magnetization, recorded under a 1 kOe field, of (a) 4−5 nm $CoFe_2O_4$ nanoparticles, (b) pure MnO nanoparticles (size 18 nm), and (c) $CoFe_2O_4$/MnO (indicated as CF/MnO) nanoparticles as a function of temperature. The nominal core/shell ratio of CF/MnO was 3:1, respectively. The pure CF particles (a) display a blocking temperature (T_B) of about 200 K. The MnO particles do not display a clear Néel temperature, expected at 118 K for bulk MnO,[12] as indicated by the vertical dashed line. At temperatures below 50 K, the MnO particles display some ZFC/FC divergence because of imperfect compensation of antiferromagnetic sublattices in nanoparticles.[13] The CF/MnO particles display behavior that is distinct from both pure CF and MnO. These composite particles show evidence for blocking as well as for the antiferromagnetic cusp at a slightly reduced (near 100 K) temperature.

Figure 3d,e displays magnetization as a function of the magnetic field acquired at 5 K after cooling from 300 K under a 10 kOe field. Such field cooling, in an interfacial system whose Curie temperature is higher than the blocking temperature, results in

10.1021/ja051244s CCC: $30.25

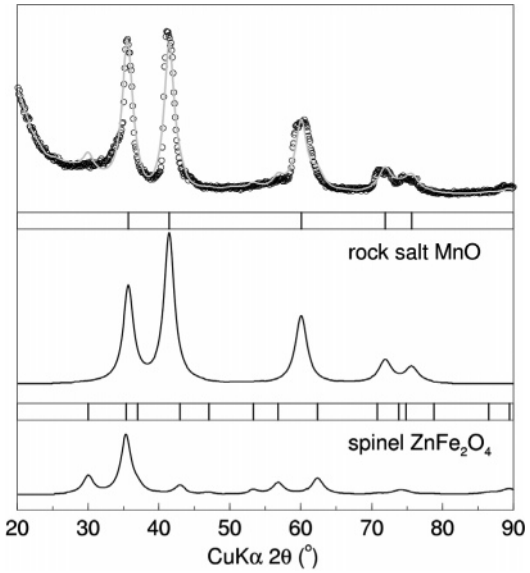

Figure 1. XRD data (open circles) and Rietveld refinement (solid lines) of $ZnFe_2O_4$/MnO nanoparticles with nominal 6:1 core:shell ratio. The panels below are the individual Rietveld fits to the rock salt MnO [$a = 4.35(1)$ Å] and $ZnFe_2O_4$ [$a = 8.41(1)$ Å] structures. Vertical lines indicate expected peak positions. From Rietveld scale factors, actual core:shell mole ratios were obtained to be close to 6:1.

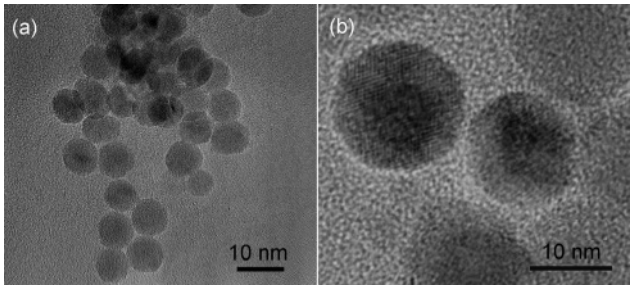

Figure 2. TEM images of 8 nm $CoFe_2O_4$/MnO nanoparticles with a nominal 3:1 core:shell ratio.

exchange biasing at the interface. From Figure 3d, it is seen that 4−5 nm CF nanoparticles have high coercivities approaching 16 kOe and saturation magnetizations near 75 emu g^{-1}. On this scale, the CF/MnO architecture has a barely perceptible hysteresis loop, and MnO is almost paramagnetic. Seen closely, the hysteresis loop of the CF/MnO particles (Figure 3d) displays a much smaller coercive field (around 2.5 kOe) as well as a smaller remanent field. Because many of the spins in the architecture are not participants in the magnetic ordering, the loop is not well-saturated. The most impressive aspect of the loop is that it is clearly shifted to negative magnetic fields, by an exchange field $H_E = 0.6$ kOe. This is evidence for exchange biasing at the ferrimagnetic/antiferromagnetic interface. The greatly reduced coercive field of the CF/MnO nanoparticles, however, suggests that during the preparative process, the CF core did not retain its chemical identity and there has perhaps been significant cation mixing between core and shell; Mn-substituted spinel ferrites are much softer than $CoFe_2O_4$.

Bulk MnO is antiferromagnetic, but recent studies have shown weak ferromagnetic behavior in nanosized MnO at low temperatures.[13−15] We have also observed ferromagnetic behavior in native MnO nanoparticles prepared according to ref 11, as seen from Figure 3b, but this is clearly not responsible for the behavior of the core/shell structure. Future work will be directed at developing synthetic conditions which ensure that the cation sublattices of core and shell remain chemically pure.

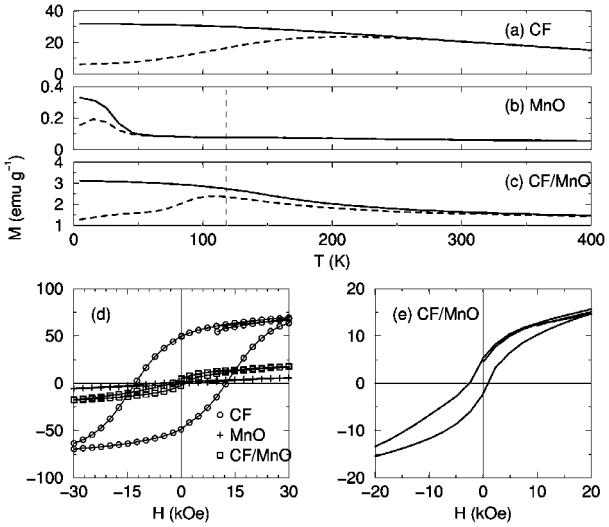

Figure 3. Magnetization under a 1 kOe field as a function of temperature (a−c) and at 5 K as a function of field acquired after cooling under a 10 kOe field (d and e). In a−c, field-cooled data (FC) are displayed as solid lines, and zero-field-cooled (ZFC) data as dashed lines. The different systems are labeled in the figure. Vertical lines in b and c are the Néel temperature of bulk MnO.

Acknowledgment. We acknowledge support from the Donors of the American Chemical Society Petroleum Research Fund and the Materials Research Laboratory, UCSB (supported by the National Science Foundation, DMR00 80034).

Supporting Information Available: Additional figures. This material is available free of charge via the Internet at http://pubs.acs.org.

References

(1) Berkowitz, A. E.; Takano, K. *J. Magn. Magn. Mater*. **1999**, *200*, 552−570.
(2) (a) Meiklejohn, W. H.; Bean, C. P. *Phys. Rev*. **1956**, *102*, 1413−1414. (b) Meiklejohn, W. H.; Bean, C. P. *Phys. Rev*. **1957**, *105*, 904−913.
(3) Nogués, J.; Schuller, I. V. *J. Magn. Magn. Mater*. **1999**, *192*, 203−232.
(4) Schuller, I. K. *MRS Bull*. **2004**, *29*, 642−646.
(5) Cai, J. W.; Kai, L.; Chien, C. L. *Phys. Rev. B* **1999**, *60*, 72−75.
(6) Skumryev, V.; Stoyanov, S.; Zhang, Y.; Hadjipanayis, G.; Givord, D.; Nogués, J. *Nature* **2003**, *423*, 850−853.
(7) Bi, H.; Li, S.; Jiang, X.; Du, Y.; Yang, C. *Phys. Lett. A* **2003**, *307*, 69−75.
(8) Masala, O.; Seshadri, R. *Annu. Rev. Mater*. **2004**, *34*, 41−81.
(9) Sun, S.; Zeng, H.; Robinson, D. B.; Raoux, S.; Rice, P. M.; Wang, S. X.; Li, G. *J. Am. Chem. Soc.* **2004**, *126*, 273−279.
(10) Masala, O.; Seshadri, R. *Chem. Phys. Lett*. **2005**, *402*, 160−164.
(11) Yin, M.; O'Brien, S. *J. Am. Chem. Soc*. **2003**, *125*, 10180−10181.
(12) Rao, C. N. R.; Subba Rao, G. V. *Transition Metal Oxides: Crystal Chemistry, Phase Transitions, and Related Aspects*; National Standard Reference Data System, National Bureau of Standards: Washington, DC, 1974.
(13) Lee, G. H.; Huh, S. H.; Jeong, J. W.; Choi, B. J.; Kim, S. H.; Ri, H.-C. *J. Am. Chem. Soc.* **2002**, *124*, 12094−12095.
(14) Seo, W. S.; Jo, H. H.; Lee, K.; Kim, B.; Oh, S. J.; Park, J. T. *Angew. Chem., Int. Ed.* **2004**, *43*, 1115−1117.
(15) Park, J.; Kang, E.; Bae, C. J.; Park, J.-G.; Noh, H.-J.; Kim, J.-Y.; Park, J.-H.; Park, H. M.; Hyeon, T. *J. Phys. Chem. B* **2004**, *108*, 13594−13598.

JA051244S